



Cite this: *Chem. Commun.*, 2014, 50, 15082

Received 22nd September 2014,  
Accepted 16th October 2014

DOI: 10.1039/c4cc07478e

www.rsc.org/chemcomm

## Effective separation of Am(III) and Eu(III) from HNO<sub>3</sub> solutions using CyMe<sub>4</sub>-BTPhen-functionalized silica-coated magnetic nanoparticles†

Ashfaq Afsar,<sup>a</sup> Laurence M. Harwood,<sup>\*a</sup> Michael J. Hudson,<sup>a</sup> Petr Distler<sup>b</sup> and Jan John<sup>b</sup>

It has been shown that CyMe<sub>4</sub>-BTPhen-functionalized silica-coated maghemite ( $\gamma$ -Fe<sub>2</sub>O<sub>3</sub>) magnetic nanoparticles (MNPs) are capable of quantitative separation of Am(III) from Eu(III) from HNO<sub>3</sub> solutions. These MNPs also show a small but significant selectivity for Am(III) over Cm(III) with a separation factor of around 2 in 4 M HNO<sub>3</sub>. The water molecule in the cavity of the BTPhen may also play an important part in the selectivity.

A key step in closing the nuclear fuel cycle may involve the partitioning and transmutation of irradiated nuclear fuel. In the case of the minor actinides (Am and Cm) this requires their selective separation from the chemically similar trivalent lanthanides.<sup>1</sup> One approach to this has resulted in the development of a combination of two partitioning processes to be applied to post PUREX raffinate. This protocol is based on the co-separation of trivalent actinides and lanthanides by a diamide-based ligand (DIAMEX) process, followed by selective separation of trivalent actinides in a SANEX (Selective ActiNide EXtraction) process.<sup>2</sup> One of the SANEX processes considered utilizes liquid–liquid extraction using nitrogen bearing ligands such as the 2,6-bis(1,2,4-triazine-3-yl)pyridines (BTPs),<sup>3–5</sup> or 6,6'-bis(1,2,4-triazin-3-yl)-2,2'-bipyridines (BTBPs)<sup>4–8</sup> (see Fig. 1) dissolved in an organic diluent.

In a recent development, the 2,2'-bipyridine moiety was replaced by a 1,10-phenanthroline moiety (BTPhens).<sup>9–13</sup> This ligand has

specific differences from the BTBPs. CyMe<sub>4</sub>-BTPhen is more pre-organized for complex formation; it has a dipole moment and so is more surface active at the interface.<sup>12</sup> Consequently CyMe<sub>4</sub>-BTPhen shows faster rates of metal ion extraction and stripping together with distribution ratios that are two orders of magnitude higher for An(III) extraction in liquid–liquid extraction experiments than its non-preorganized BTBP counterpart.<sup>12</sup>

However, selective extraction of minor actinides by a liquid–liquid extraction process comes with certain disadvantages, such as the requirement for substantial liquid storage and containment and generation of significant amounts of secondary waste.<sup>14,15</sup> Thus there is a requirement for new systems that are capable of polishing the raffinates from the SANEX and related processes as well as for dealing with low level activity of liquid wastes.

Recently magnetic separation technology has attracted attention in the area of spent nuclear fuel separation.<sup>14,16</sup> It is proposed that when magnetic nanoparticles (MNPs) are combined with ligands such as CyMe<sub>4</sub>-BTPhen, these functionalized MNPs could be used to extract the minor actinides and the radioactive material could then be collected magnetically in preference to centrifugation. Finally, the MNPs could be recycled by stripping the radioactive elements from the conjugates, generating a very small amount of secondary waste.

Owing to the acidic nature of the post-PUREX aqueous raffinate (typically 4 M HNO<sub>3</sub>), unmodified iron or iron oxide based MNPs cannot be used in this medium. It was proposed to solve this problem by using a silica coating in order to provide a chemically unreactive surface to the MNPs whilst not affecting the core.<sup>17,18</sup> Furthermore, the free Si–OH surface groups can allow effective covalent binding of organic functional groups.<sup>17,18</sup> In the work reported herein, we have investigated the separation of minor actinides from lanthanides using CyMe<sub>4</sub>-BTPhen-functionalized SiO<sub>2</sub>-coated MNPs.

Iodoalkyl-functionalized SiO<sub>2</sub>-coated MNP 3 was prepared according to our previous work.<sup>17</sup> Iron oxide ( $\gamma$ -Fe<sub>2</sub>O<sub>3</sub>) MNPs were freshly prepared<sup>19–21</sup> and the protective silica layer was then coated onto the surface of the MNPs by a sol–gel procedure.<sup>19–21</sup>

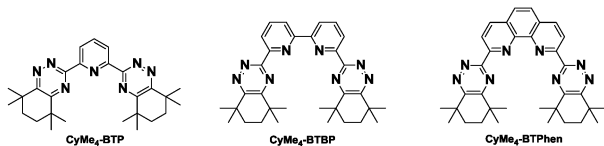


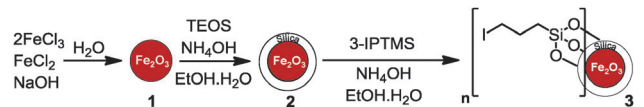
Fig. 1 Structures of CyMe<sub>4</sub>-BTP, CyMe<sub>4</sub>-BTBP and CyMe<sub>4</sub>-BTPhen.

<sup>a</sup> School of Chemistry, University of Reading, Whiteknights, Reading, Berkshire RG6 6AD, UK. E-mail: l.m.harwood@reading.ac.uk

<sup>b</sup> Department of Nuclear Chemistry, Czech Technical University in Prague, Břehová 7, 11519 Prague 1, Czech Republic. E-mail: jan.john@jfifi.cvut.cz

† Electronic supplementary information (ESI) available. See DOI: 10.1039/c4cc07478e



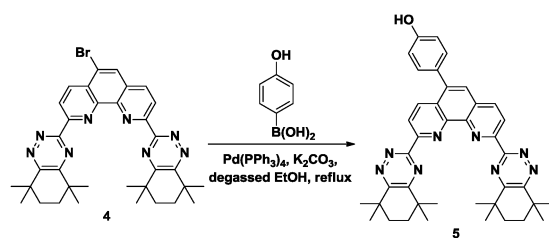
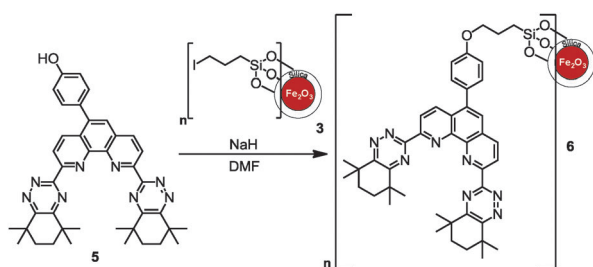
Scheme 1 Synthesis of iodoalkyl-functionalized SiO<sub>2</sub>-coated MNPs **3**.<sup>17</sup>

Subsequently, the silica surface was modified with 3-iodopropyltrimethoxysilane (3-IPMS) (Scheme 1).

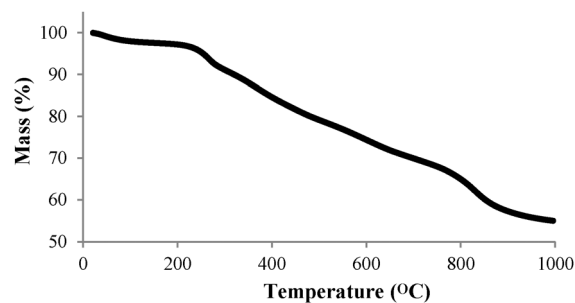
The 5-BrCyMe<sub>4</sub>-BTPPhen ligand **4** was synthesized by a protocol previously described<sup>11</sup> with the modification that the final step was performed using tetramethylcyclohexane-1,2-dione. Replacement of the bromine with a 4-hydroxyphenyl linking group was successfully achieved by Suzuki coupling<sup>22</sup> with 4-hydroxyphenylboronic acid to give **5** (Scheme 2). This 5-(4-hydroxyphenyl) functionalized CyMe<sub>4</sub>-BTPPhen ligand **5** was then immobilized onto the iodoalkyl-functionalized SiO<sub>2</sub>-coated MNP **3** by nucleophilic substitution (Scheme 3).

Each surface modification step was followed by FT-IR (ESI<sup>†</sup>), demonstrating a clear distinction between iodoalkyl-functionalized SiO<sub>2</sub>-coated MNP **3** and CyMe<sub>4</sub>-BTPPhen-functionalized SiO<sub>2</sub>-coated MNP **6**. Absence of the C–I stretching at 688 cm<sup>-1</sup> and presence of bands at 1500–1600 cm<sup>-1</sup> owing to C=C aromatic vibrations are indicative of the covalent incorporation of CyMe<sub>4</sub>-BTPPhen onto the MNP.

Elemental analysis was also used to evaluate surface incorporation of 3-IPMS in **3** and also the composition of the target CyMe<sub>4</sub>-BTPPhen-functionalized MNP **6**. Percentages of C, H, N and I in iodoalkyl-functionalized SiO<sub>2</sub>-coated MNP **3** and CyMe<sub>4</sub>-BTPPhen-functionalized SiO<sub>2</sub>-coated MNP **6** are shown in Table 1. Immobilization of CyMe<sub>4</sub>-BTPPhen onto the surface of the SiO<sub>2</sub>-coated MNP was confirmed on the basis of the presence of nitrogen in **6** but not in **3** (*i.e.* 3.43% for CyMe<sub>4</sub>-BTPPhen-functionalized SiO<sub>2</sub>-coated MNP **6** and 0.10% for iodoalkyl-functionalized SiO<sub>2</sub>-coated MNP **3**). Elemental analysis also indicated that

Scheme 2 Synthesis of 5-phenol-CyMe<sub>4</sub>-BTPPhen **5**.Scheme 3 Immobilisation of CyMe<sub>4</sub>-BTPPhen on MNPs.Table 1 Results of elemental analysis for iodoalkyl-functionalized SiO<sub>2</sub>-coated MNP **3** and CyMe<sub>4</sub>-BTPPhen-functionalized SiO<sub>2</sub>-coated MNP **6**

	Iodoalkyl-functionalized SiO <sub>2</sub> -coated MNP <b>3</b>		CyMe <sub>4</sub> -BTPPhen-functionalized SiO <sub>2</sub> -coated MNP <b>6</b>	
	Experimental	Theoretical	Experimental	Theoretical
C (%)	11.59	10.66	23.20	22.79
H (%)	2.50	1.79	3.48	2.14
N (%)	0.10	0	3.43	4.94
I (%)	38.92	37.54	8.28	0

Fig. 2 TGA curve of MNP **6**.

the surface modification of iodoalkyl-functionalized SiO<sub>2</sub>-coated MNP **3** with 5-phenol-CyMe<sub>4</sub>-BTPPhen ligand **5** had resulted in a *ca.* 80% of the iodoalkyl groups being successfully substituted.

The organic content on the MNPs was further investigated using thermal gravimetric analysis (TGA) under nitrogen (Fig. 2). Below 150 °C, the mass loss is quite small, probably corresponding to removal of absorbed water. After that, there is a more-or-less linear mass loss between *ca.* 250–700 °C corresponding to decomposition of the organic components. From this, it can be estimated that the amount of CyMe<sub>4</sub>-BTPPhen bound onto the MNP is about *ca.* 20% w/w (ESI<sup>†</sup>). Further mass loss above *ca.* 800 °C can be attributed to the loss of carbon – perhaps during the formation of iron carbide.<sup>23,24</sup>

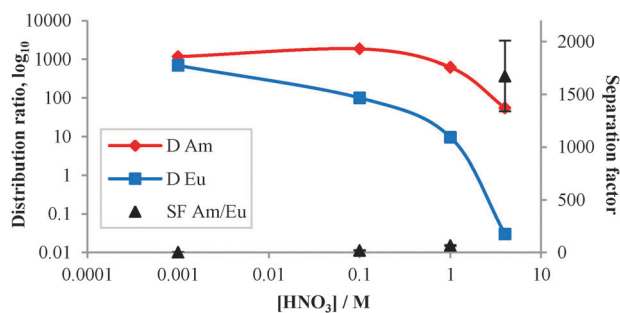
The aqueous solutions for the solvent extraction experiments were prepared by spiking nitric acid solutions (0.001–4 M) with stock solutions of <sup>241</sup>Am, <sup>152</sup>Eu and <sup>244</sup>Cm and then adding 600 μL of spiked aqueous solution to 18 mg of CyMe<sub>4</sub>-BTPPhen-functionalized MNP **6**. The suspension was sonicated for 10 min and shaken at 1800 rpm for 90 min. After centrifuging for 10 min, aliquots of the aqueous solutions (supernatant) were separated and taken for measurements. The distribution ratios, *D*, were calculated as the ratio between the radioactivity ( $\alpha$ - and  $\gamma$ -emissions) of each isotope in the standard solution and the supernatants after removal of MNP **6**. The separation factor is  $SF_{Am/Eu} = D_{Am}/D_{Eu}$  or  $SF_{Am/Cm} = D_{Am}/D_{Cm}$  (Table 2).

Extractions were studied at nitric acid concentrations of 0.001 M, 0.1 M, 1 M and particularly 4 M. The distribution ratios and separation factors for the extraction of Am(III) and Eu(III) from nitric acid solutions at these concentrations are shown in Fig. 3. High distribution ratios ( $D > 700$ ) were obtained for both Am(III) and Eu(III) at 0.001 M HNO<sub>3</sub> solution with no significant selectivity ( $SF_{Am/Eu} = 1.7 \pm 0.1$ ) for Am(III) over Eu(III). At 0.1 M HNO<sub>3</sub>, the *D* value for Am(III) remained



**Table 2** Extraction of Am(III) and Eu(III) by MNP **6** as a function of nitric acid concentration

[HNO <sub>3</sub> ]	<i>D</i> <sub>Am</sub>	<i>D</i> <sub>Eu</sub>	SF <sub>Am/Eu</sub>
0.001	1162.8 ± 79.1	701.4 ± 32.4	1.7 ± 0.1
0.1	1857.0 ± 153.5	101.1 ± 2.3	18.4 ± 1.6
1	623.1 ± 31.2	9.6 ± 0.6	65.2 ± 5.0
4	55.4 ± 1.5	0.03 ± 0.4	1675.6 ± 335.1

**Fig. 3** Extraction of Am(III) and Eu(III) by MNP **6** as a function of nitric acid concentration.

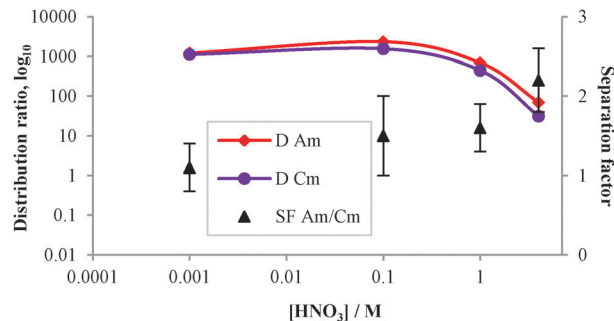
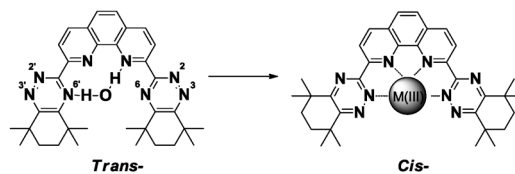
high ( $D_{\text{Am}} = 1857 \pm 153.5$ ), but the  $D$  value for Eu(III) was significantly lower ( $D_{\text{Eu}} = 101 \pm 2.3$ ), resulting in  $\text{SF}_{\text{Am/Eu}} = 18.4 \pm 1.6$ . Decreases in the  $D$  values for both Am(III) and Eu(III) were observed ( $D_{\text{Am}} = 623.1 \pm 31.2$ ,  $D_{\text{Eu}} = 9.6 \pm 0.6$ ) at 1 M HNO<sub>3</sub> solution, but a higher separation factor ( $\text{SF}_{\text{Am/Eu}} = 65.2 \pm 5$ ) resulted. Finally, at 4 M HNO<sub>3</sub> a further decrease in  $D$  value for Am(III) gave  $D_{\text{Am}} = 55.4 \pm 1.5$  but, in this case the  $D$  value observed for Eu(III) of  $D_{\text{Eu}} = 0.03 \pm 0.4$ , meant that only Am(III) was retained on the MNP **6**. The resulting separation factor ( $\text{SF}_{\text{Am/Eu}} =$  estimated to be  $>1300$ ) is far superior to that observed for CyMe<sub>4</sub>-BTPhen ( $\text{SF}_{\text{Am/Eu}} = 400$ )<sup>9,10</sup> in solvent extraction experiments under similar conditions and means that quantitative separation of Am(III) from Eu(III) is possible at this concentration of HNO<sub>3</sub> (Table 3).

Distribution ratios for Am(III) and Cm(III), and the separation factors at different nitric acid concentrations were also examined (Fig. 4). The  $D$  values for both Am(III) and Cm(III) decreased with increasing nitric acid concentration, in agreement with the earlier results, resulting in a small but significant  $\text{SF}_{\text{Am/Cm}} = 2.2 \pm 0.4$  at 4 M HNO<sub>3</sub>.

We propose that the shortness of the linking-chain on the MNP constrains the CyMe<sub>4</sub>-BTPhen ligand to form 1:1 complexes with M(III) cations.<sup>25</sup> For the quadridentate CyMe<sub>4</sub>-BTPhen ligand, the dominant metal–ligand complex stoichiometry in solution is 1:2 however, species proposed to be 1:1

**Table 3** Extraction of Am(III) and Cm(III) by MNP **6** as a function of nitric acid concentration

[HNO <sub>3</sub> ]	<i>D</i> <sub>Am</sub>	<i>D</i> <sub>Cm</sub>	SF <sub>Am/Cm</sub>
0.001	1212.9 ± 204.4	1117.4 ± 195.6	1.1 ± 0.3
0.1	2348.8 ± 525.7	1561.1 ± 331.5	1.5 ± 0.5
1	690.7 ± 88.2	444.1 ± 50.7	1.6 ± 0.3
4	69.6 ± 4.8	31.4 ± 2.9	2.2 ± 0.4

**Fig. 4** Extraction of Am(III) and Cm(III) by MNP **6** as a function of nitric acid concentration.**Fig. 5** Preferred rotamer of [M(III)CyMe<sub>4</sub>-BTPhen].<sup>9,12</sup>

complexes can be observed by <sup>1</sup>H-NMR titrations at high Ln(III) loadings and a crystal of a 1:1 complex [Y(CyMe<sub>4</sub>-BTPhen)(NO<sub>3</sub>)<sub>3</sub>]. MeCN has been isolated and structurally characterized in the solid state.<sup>12,26</sup> In the crystal, the yttrium(III) cation is 10-coordinate being bonded to the tetradentate CyMe<sub>4</sub>-BTPhen and to three bidentate nitrate ions.

In the BTPhen moiety, the strongly bound water molecule in the central cavity may also play an important role in the separation of Am(III) from Eu(III). The initial attack of the cation is probably on the N(2) of the triazine ring in the *trans*-rotamer (Fig. 5). This bound metal then seeks to bind with other nitrogens and as the *cis*-rotamer is forming, the strongly bound water molecule is displaced. The Am(III) subsequently binds to all four nitrogen atoms in the BTPhen, while the Eu(III) cations are unable to bind, particularly at higher nitric acid concentrations, thus providing for the quantitative separation of Am(III) from Eu(III). Further studies into this proposed mechanism are continuing.

In summary, the CyMe<sub>4</sub>-BTPhen ligand has been covalently bound to SiO<sub>2</sub>-coated MNPs by a phenyl ether linkage after functionalization at C-5 of the phenanthroline. The MNP **4** exhibits very high selectivity for Am(III) over Eu(III) at 4 M HNO<sub>3</sub> (with a separation factor in excess of 1300). This MNP also shows a small but significant selectivity for Am(III) over Cm(III) with a nominal separation factor of around 2 in 4 M HNO<sub>3</sub>. We propose that this technology may well prove effective for polishing the raffinate from SANEX-type processes and for remediation of contaminated water or soils.

The authors acknowledge the EPSRC for financial support (A.A.). Use of the Chemical Analysis Facility (CAF) and Centre for Advanced Microscopy (CfAM) at the University of Reading is also gratefully acknowledged. We also would like to thank Dr Peter Harris for his assistance with Transmission Electron Microscopy (TEM).



## Notes and references

- 1 F. W. Lewis, L. M. Harwood, M. J. Hudson, P. Distler, J. John, K. Stamberg, A. Núñez, H. Galán and A. G. Espartero, *Eur. J. Org. Chem.*, 2012, 1509–1519.
- 2 A. Fermvik, C. Ekberg, S. Englund, M. R. S. J. Foreman, G. Modolo, T. Retegan and G. Skarnemark, *Radiochim. Acta*, 2009, **97**, 319–324.
- 3 M. Weigl, A. Geist, U. Müllich and K. Gompfer, *Solvent Extr. Ion Exch.*, 2006, **24**, 845–860.
- 4 P. J. Panak and A. Geist, *Chem. Rev.*, 2013, **113**, 1199–1236.
- 5 F. W. Lewis, M. J. Hudson and L. M. Harwood, *Synlett*, 2011, 2609–2632.
- 6 M. Nilsson, C. Ekberg, M. Foreman, M. Hudson, J. O. Liljenzin, G. Modolo and G. Skarnemark, *Solvent Extr. Ion Exch.*, 2006, **24**, 823–843.
- 7 E. Aneheim, B. Grüner, C. Ekberg, M. R. S. Foreman, Z. Hájková, E. Löfström-Engdahl, M. G. B. Drew and M. J. Hudson, *Polyhedron*, 2013, **50**, 154–163.
- 8 D. Magnusson, B. Christiansen, M. R. S. Foreman, A. Geist, J. P. Glatz, R. Malmbeck, G. Modolo, D. Serrano-Purroy and C. Sorel, *Solvent Extr. Ion Exch.*, 2009, **27**, 97–106.
- 9 F. W. Lewis, L. M. Harwood, M. J. Hudson, M. G. Drew, J. F. Desreux, G. Vidick, N. Bouslimani, G. Modolo, A. Wilden, M. Sypula, T. H. Vu and J. P. Simonin, *J. Am. Chem. Soc.*, 2011, **133**, 13093–13102.
- 10 F. W. Lewis, L. M. Harwood, M. J. Hudson, M. G. B. Drew, A. Wilden, M. Sypula, G. Modolo, T.-H. Vu, J.-P. Simonin, G. Vidick, N. Bouslimani and J. F. Desreux, *Procedia Chem.*, 2012, **7**, 231–238.
- 11 A. Afsar, D. M. Laventine, L. M. Harwood, M. J. Hudson and A. Geist, *Chem. Commun.*, 2013, **49**, 8534–8536.
- 12 F. W. Lewis, L. M. Harwood, M. J. Hudson, M. G. B. Drew, V. Hubscher-Bruder, V. Videva, F. Arnaud-Neu, K. Stamberg and S. Vyas, *Inorg. Chem.*, 2013, **52**, 4993–5005.
- 13 D. M. Laventine, A. Afsar, M. J. Hudson and L. M. Harwood, *Heterocycles*, 2012, **86**, 1419–1429.
- 14 M. Kaur, A. Johnson, G. Tian, W. Jiang, L. Rao, A. Paszczynski and Y. Qiang, *Nano Energy*, 2013, **2**, 124–132.
- 15 M. Kaur, H. Zhang, L. Martin, T. Todd and Y. Qiang, *Environ. Sci. Technol.*, 2013, **47**, 11942–11959.
- 16 A. Afsar, D. M. Laventine, L. M. Harwood, M. J. Hudson and A. Geist, *Heterocycles*, 2014, **88**, 613.
- 17 A. Afsar, L. M. Harwood, M. J. Hudson, M. E. Hodson and E. J. Shaw, *Chem. Commun.*, 2014, **50**, 7477–7480.
- 18 J. H. Jang and H. B. Lim, *Microchem. J.*, 2010, **94**, 148–158.
- 19 A. L. Morel, S. I. Nikitenko, K. Gionnet, A. Wattiaux, J. Lai-Kee-Him, C. Labrugere, B. Chevalier, G. Deleris, C. Petibois, A. Brisson and M. Simonoff, *ACS Nano*, 2008, **2**, 847–856.
- 20 M. Nazrul Islam, L. Van Phong, J.-R. Jeong and C. Kim, *Thin Solid Films*, 2011, **519**, 8277–8279.
- 21 F. W. Zhang, Z. Z. Zhu, Z. P. Dong, Z. K. Cui, H. B. Wang, W. Q. Hu, P. Zhao, P. Wang, S. Y. Wei, R. Li and J. T. Ma, *Microchem. J.*, 2011, **98**, 328–333.
- 22 J. P. W. Eggert, U. Luning and C. Nather, *Eur. J. Org. Chem.*, 2005, 1107–1112.
- 23 R. Snovski, J. Grinblat, M.-T. Sougrati, J.-C. Jumas and S. Margel, *J. Magn. Magn. Mater.*, 2014, **349**, 35–44.
- 24 M. Sharma, S. Mantri and D. Bahadur, *J. Magn. Magn. Mater.*, 2012, **324**, 3975–3980.
- 25 M. J. Hudson and Z. Matejka, *Sep. Sci. Technol.*, 1989, **24**, 1417–1426.
- 26 D. M. Whittaker, T. L. Griffiths, M. Helliwell, A. N. Swinburne, L. S. Natrajan, F. W. Lewis, L. M. Harwood, S. A. Parry and C. A. Sharrad, *Inorg. Chem.*, 2013, **52**, 3429–3444.

